Acta Cryst E CRYSTALLOGRAPHIC COMMUNICATIONS

ISSN 2056-9890

Crystal structure and Hirshfeld surface analysis of 3,3′-(sulfanediyl)bis(2-iodo-1-methyl-1*H*-indole)

Adisa Ayobami,[a] Abid Shaikh[a] and Clifford W. Padgett[b]*

[a]Georgia Southern University, 521 College of Education Dr., Department of Chemistry, Biochemistry and Physics, Statesboro, GA 30458, USA, and [b]Georgia Southern University, 11935 Abercorn St., Department of Chemistry, Biochemistry and Physics, Savannah, GA 31419, USA. *Correspondence e-mail: cpadgett@georgiasouthern.edu

Received 16 January 2026
Accepted 18 March 2026

Edited by F. F. Ferreira, Universidade Federal do ABC, Brazil

Keywords: bis(indolyl)sulfane; synthesis; crystal structure.

CCDC reference: 2539020

Supporting information: this article has supporting information at journals.iucr.org/e

The title compound, $C_{18}H_{14}I_2N_2S$, comprises two *N*-methyl-2-iodoindole fragments linked at the 3-positions by a thioether bridge. The sulfur atom adopts a typical thioether geometry, and the C—S—C linkage is *gauche* on both sides, with C—S—C—C torsion angles of −64.1 (11) and −48.3 (10)°. The indole units are essentially planar and are strongly inclined to one another, with an interplanar angle of 103.3 (3)°. The compound crystallizes in the orthorhombic space group *Fdd2*; the molecule lacks classical hydrogen-bond donors, and no significant hydrogen bonding or π–π stacking is observed. The packing is dominated by van der Waals interactions together with short I···C and I···π contacts, giving a herringbone arrangement and forming chains along the *b* axis. Hirshfeld surface analysis indicates that H···H (33.1%), H···C/C···H (25.5%) and H···I/I···H (24.4%) contacts make the largest contributions to the crystal packing.

1. Chemical context

Sulfur-bridged indolyl compounds have attracted interest because of their relevance to medicinal chemistry (Xalxo *et al.*, 2023; Silveira *et al.*, 2013) and materials science (Yuan *et al.*, 2022), as well as their ability to serve as versatile synthons in organic chemistry (Wang, 2024). Diarylated thioethers (aryl–S–aryl motifs) are used in functional materials; for example, thioether-linked polymeric systems have been developed for adsorption/capture applications such as iodine uptake (Shetty *et al.*, 2022), and porous poly(aryl thioether) frameworks have also been explored for metal capture, sensing, and heterogeneous catalysis (Rivero-Crespo *et al.*, 2021). Thienoindole-based π-systems have also been incorporated into conjugated polymers for organic electronic applications (Jeong *et al.*, 2016). The motivation for studying these motifs comes from the central role of indole scaffolds in drug discovery (Mo *et al.*, 2024) and from literature reports that indole-based aryl sulfides can exhibit potent antibacterial activity against *Staphylococcus aureus* (Lavekar *et al.*, 2024). Organosulfur compounds containing thioether (sulfane) linkages are known to influence molecular conformation, electronic properties, and intermolecular interactions in the solid state (Gundermann, 1963). Incorporation of a sulfide bridge between two indole moieties can enhance structural rigidity while allowing conformational flexibility about the C–S–C linkage (Mohanty *et al.*, 2025). The presence of iodine atoms at the 2-position of the indole rings provides opportunities for specific intermolecular contacts, while *N*-methylation suppresses classical N—H hydrogen bonding, allowing a clearer assessment of the roles played by halogen···halogen, halogen···π, and sulfur-involved interactions in the crystal structure (Bergman & Janosik, 2002). 3,3′-Sulfanediylbis(2-iodo-1-methyl-1*H*-

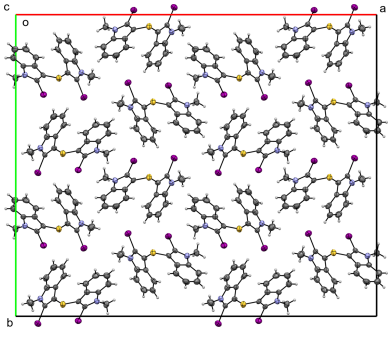

indole) serves as a model system for assessing I···I, I···π and sulfur-involving contacts in the absence of classical hydrogen-bond donors, providing guidance for the crystal engineering of closely related derivatives. Herein, we report its synthesis and single-crystal X-ray diffraction analysis.

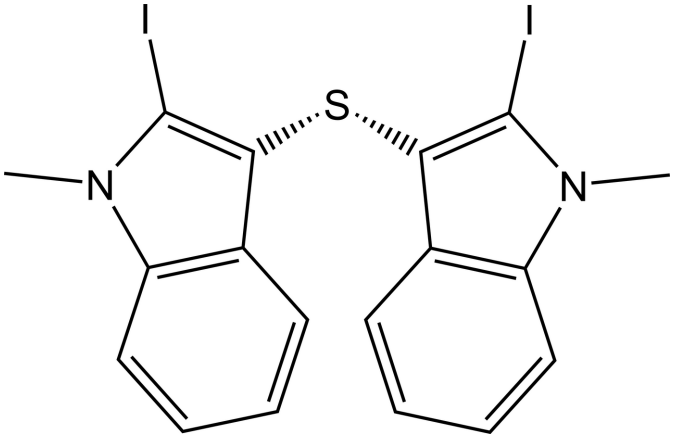

2. Structural commentary

The molecular structure of 3,3′-sulfanediylbis(2-iodo-1-methyl-1*H*-indole), (**I**), consists of two *N*-methyl-2-iodoindole fragments linked through a thioether bridge at the 3-position (Fig. 1). The C—I bond lengths are similar [I1—C1 = 2.079 (12) Å and I2—C10 = 2.080 (9) Å]. The sulfur atom adopts a typical thioether geometry with S1—C2 = 1.761 (11) Å and S1—C11 = 1.770 (11) Å, and a C2—S1—C11 angle of 100.6 (5)°. The conformation about the S bridge is *gauche* on both sides, as shown by the torsion angles C11—S1—C2—C1 = −64.1 (11)° and C2—S1—C11—C12 = −48.3 (10)°. Both indole ring systems are essentially planar, with r.m.s. deviations of 0.012 Å for the N1/C1–C8 system and 0.017 Å for the N2/C10–C17 system. The two indole mean planes are strongly inclined, with an interplanar angle (normal-to-normal) of 76.3 (3)°.

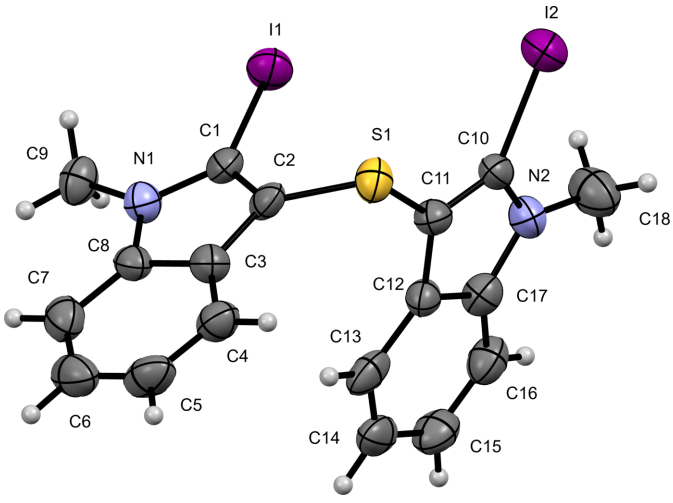

Figure 1
The molecular structure of (**I**) with displacement ellipsoids drawn at the 50% probability level.

3. Supramolecular features

Compound (I) crystallizes in the orthorhombic space group *Fdd*2. In the crystal, the molecule lacks classical hydrogen-bond donors and no significant hydrogen-bonding interactions are observed; likewise, no π–π stacking between indole rings is evident. The packing (Fig. 2) is dominated primarily by van der Waals contacts, but with shorter than van der Waals intermolecular I···C contacts, C14···I1^{i} = 3.341 (12) Å and C5···I2^{i} = 3.433 (14) Å [symmetry code: (i) $\frac{3}{4} - x, \frac{1}{4} + y, -\frac{1}{4} + z$]. The molecules pack in a herringbone pattern with each iodine substituent oriented toward the six-membered π-system of an indole ring in a neighbouring, symmetry-related molecule, giving rise to I···π contacts. For I1, the perpendicular separation from the plane of the C12–C17 ring is 3.217 (13) Å and the iodine-to-centroid distance is I1···*Cg*(C12–C17)^{i} = 3.906 (5) Å; the C1—I1 vector makes an angle of 152.7 (4)° with the ring-plane normal and the C1—I1···*Cg*^{i} angle is 166.8 (3)°. Similarly, I2 lies 3.323 (14) Å from the plane of the C3–C8 ring with I2···*Cg*(C3–C8)^{i} = 3.999 (5) Å; the C10–I2 vector makes an angle of 25.0 (4)° with the ring-plane normal and the C10—I2···*Cg*^{i} angle is 171.2 (3)°. These I···π contacts link the molecules into chains running parallel to the *b* axis.

4. Hirshfeld surface analysis

The intermolecular interactions were further investigated by quantitative analysis of the Hirshfeld surface, and visualized with *Crystal Explorer 21.5* (Spackman *et al.*, 2021) and the two-dimensional fingerprint plots (McKinnon *et al.*, 2007). The

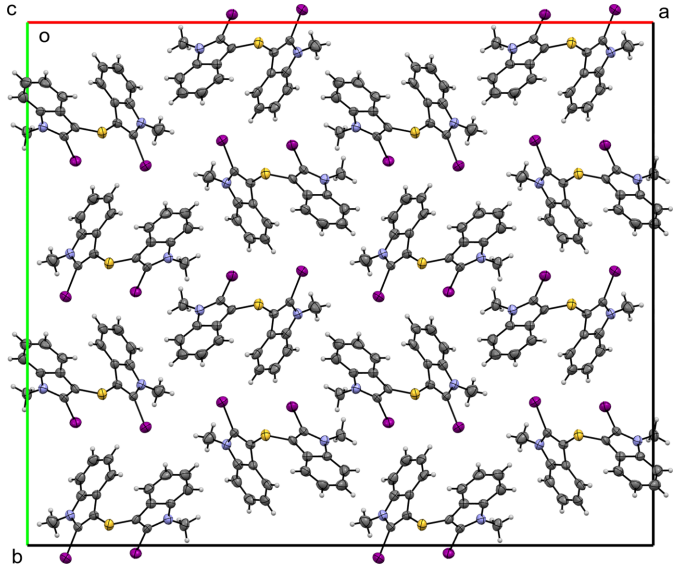

Figure 2
A view along the *c*-axis direction of the crystal packing of (**I**)

Table 1
Contributions of selected intermolecular contacts (%) to the Hirshfeld surfaces of (I).

Contact	(%)
H···H	33.1
H···C/C···H	25.5
H···I/I···H	24.4
C···I/I···C	5.2
H···S/S···H	4.9
H···N/N···H	2.6
I···S/S···I	1.7
C···S/S···C	1.4
S···N/N···S	0.9
I···I	0.2

shorter and longer contacts are indicated as red and blue spots, respectively, on the Hirshfeld surfaces, and contacts with distances approximately equal to the sum of the van der Waals radii are colored white. The function d_{norm} is a ratio enclosing the distances of any surface point to the nearest interior (d_i) and exterior (d_e) atom and the van der Waals (vdW) radii of the atoms. The d_{norm} plots were mapped with a color scale between −0.19 a.u. (red) and +1.2 a.u. (blue).

Fig. 3 shows the d_{norm} Hirshfeld surface of the title compound. The most intense red regions on the surface correspond to short intermolecular contacts involving H···I and H···C interactions, indicating their importance in the crystal packing. No pronounced red–blue triangular features are observed on the shape-index surface, suggesting the absence of significant π–π stacking interactions. Analysis of the two-dimensional fingerprint plots reveals that H···H contacts make the largest contribution to the Hirshfeld surface (33.1%), highlighting the dominant role of van der Waals interactions in the packing. This is followed by H···C/C···H (25.5%) and H···I/I···H (24.4%) interactions, which together account for a substantial fraction of the intermolecular contacts. Smaller contributions arise from C···I/I···C (5.2%), H···S/S···H (4.9%), and H···N/N···H (2.6%) contacts, while all remaining interactions contribute less than 2% individually, see Table 1.

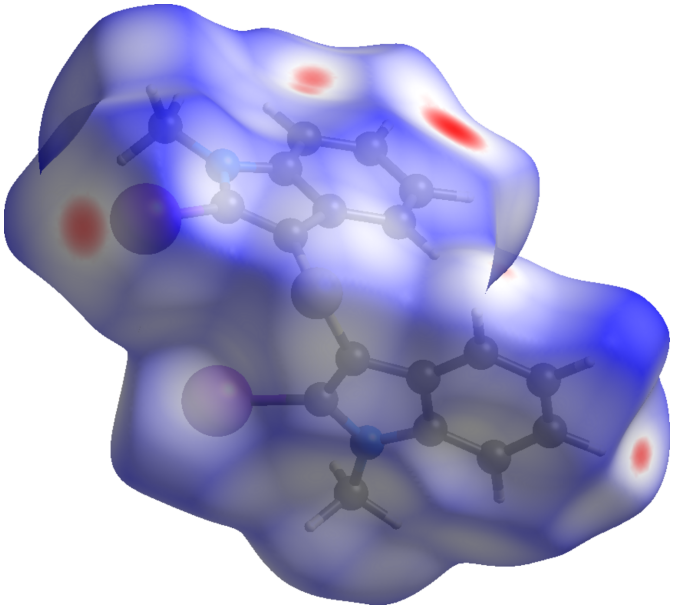

Figure 3
Hirshfeld surface for (**I**) mapped over d_{norm}.

5. Database survey

A search of the Cambridge Structural Database (CSD; website, accessed on 6 January 2026; Groom *et al.*, 2016) for structures related to the title compound, 3,3′-sulfanediylbis(2-iodo-1-methyl-1*H*-indole), returned nine relevant entries. Three structures feature the 3,3′-thioether-linked bis(indole) motif: GETCAK, 1,1′-bis(*t*-butyldimethylsilyl)-3,3′-bis(1*H*-indol-3-yl)sulfide (Shirani *et al.*, 2006), LOJTOX, 3,3′-sulfanediylbis(2-methyl-1*H*-indole) (Sharma *et al.*, 2024), and YIQPEV, 3,3′-sulfanediylbis(1-methyl-1*H*-indole) (Shibahara *et al.*, 2014); among these, YIQPEV is the closest analogue in terms of *N*-methylation, but it lacks the 2-iodo substitution present in the title compound. The remaining entries comprise iodinated indole derivatives with differing substitution patterns and functionalization, including JEVQOR, 2,3-diiodo-1-(phenylsulfonyl)-1*H*-indole (Rinderspacher *et al.*, 2007), KAGQIV, 2-iodo-1-phenyl-1*H*-indole (Messaoud *et al.*, 2015), iodoindole benzamide derivatives KAGGEJ and KAGGIN (Kim *et al.*, 2025), and 2-iodo-3-[(trifluoromethyl) selanyl]indole derivatives KOYFAJ and KOYFIR (Huang *et al.*, 2024).

6. Synthesis and crystallization

Di-*tert*-butyl disulfide (200 mg, 1.12 mmol) and *N*-methyl indole (147 mg, 1.12 mmol) were placed in a round-bottomed flask along with 2 mL of DMSO. The mixture was flushed with argon and iodine (710 mg, 2.8 mmol) and one drop of DBU (1,8-diazabicyclo[5.4.0]undec-7-ene) were added successively. The reaction mixture was then allowed to stir at room temperature for 12 h. After satisfactory conversion as indicated on TLC (10% ethyl acetate: hexane), the reaction mixture was washed with dilute sodium thiosulfate and the product was extracted in ethyl acetate. The crude product was subjected to purification using column chromatography to obtain a white solid (200 mg, 66%). Crystals for X-ray analysis were obtained by slow evaporation from ethyl acetate solution at room temperature.

Spectroscopic data: ^{1}H NMR (400 MHz, $CDCl_3$) δ = 7.75 (*d*, *J* = 6.3 Hz, 2H), 7.27 (*m*, 2H), 7.15 (*m*, 4H), 3.78 (*s*, 6H). ^{13}C NMR (101 MHz, $CDCl_3$) δ = 138.8, 129.6, 122.2, 120.1, 119.9, 112.6, 109.7, 97.12, 35.1.

7. Refinement

Crystal data, data collection and structure refinement details are summarized in Table 2. H atoms were positioned geometrically (C—H = 0.93–0.96 Å) and refined as riding with U_{iso}(H) = 1.2U_{eq}(C) or 1.5U_{eq}(Cmethyl).

Acknowledgements

The authors thank the Department of Biochemistry, Chemistry, and Physics at Georgia Southern University for the financial support of this work and the National Science Foundation Major Research Instrumentation fund for the purchase of the X-ray diffractometer.

Funding information

Funding for this research was provided by: NSF Major Research Instrumentation (MRI) program (grant No. 2215812).

Table 2
Experimental details.

Crystal data	
Chemical formula	$C_{18}H_{14}I_2N_2S$
M_r	544.17
Crystal system, space group	Orthorhombic, *Fdd*2
Temperature (K)	298
a, *b*, *c* (Å)	37.8416 (4), 31.6009 (3), 5.94404 (5)
V (Å^3)	7108.05 (11)
Z	16
Radiation type	Cu $K\alpha$
μ (mm^{-1})	28.89
Crystal size (mm)	0.15 × 0.05 × 0.02
Data collection	
Diffractometer	XtaLAB Synergy, Single source at home/near, HyPix3000
Absorption correction	Multi-scan (*CrysAlis PRO*; Rigaku OD, 2023)
T_{min}, T_{max}	0.401, 1.000
No. of measured, independent and observed [$I > 2\sigma(I)$] reflections	9127, 2434, 2352
R_{int}	0.099
(sin $\theta/\lambda)_{max}$ (Å^{-1})	0.608
Refinement	
$R[F^2 > 2\sigma(F^2)]$, $wR(F^2)$, S	0.052, 0.146, 1.18
No. of reflections	2434
No. of parameters	210
No. of restraints	1
H-atom treatment	H-atom parameters constrained
$\Delta\rho_{max}$, $\Delta\rho_{min}$ (e Å^{-3})	0.90, −1.60
Absolute structure	Flack *x* determined using 558 quotients $[(I^+)-(I^-)]/[(I^+)+(I^-)]$ (Parsons *et al.*, 2013)
Absolute structure parameter	−0.034 (16)

Computer programs: *CrysAlis PRO* (Rigaku OD, 2023), *SHELXL2018/3* (Sheldrick, 2015) and *OLEX2* (Dolomanov *et al.*, 2009).

References

Bergman, J. & Janosik, T. (2002). *Prog. Heterocycl. Chem.* **14**, 1–18.
Dolomanov, O. V., Bourhis, L. J., Gildea, R. J., Howard, J. A. K. & Puschmann, H. (2009). *J. Appl. Cryst.* **42**, 339–341.
Groom, C. R., Bruno, I. J., Lightfoot, M. P. & Ward, S. C. (2016). *Acta Cryst.* B**72**, 171–179.
Gundermann, K. D. (1963). *Angew. Chem. Int. Ed. Engl.* **2**, 674–683.
Huang, Y., Zhang, Z., Wang, H. & Weng, Z. (2024). *Org. Chem. Front.* **11**, 3968–3973.
Jeong, I., Kim, J., Kim, J., Lee, J., Lee, D. Y., Kim, I., Park, S. H. & Suh, H. (2016). *Synth. Met.* **213**, 25–33.
Kim, A., Cho, H.-A., Oh, B., Song, J. & Kwon, Y. (2025). *Commun. Chem.* **8**, 190.
Lavekar, A. G., Thakare, R., Saima, Equbal, D., Chopra, S. & Sinha, A. K. (2024). *Drug Dev. Res.* **85**, e22123.
McKinnon, J. J., Jayatilaka, D. & Spackman, M. A. (2007). *Chem. Commun.* pp. 3814–3816.
Messaoud, M. Y. A., Bentabed-Ababsa, G., Hedidi, M., Derdour, A., Chevallier, F., Halauko, Y. S., Ivashkevich, O. A., Matulis, V. E., Picot, L., Thiéry, V., Roisnel, T., Dorcet, V. & Mongin, F. (2015). *Beilstein J. Org. Chem.* **11**, 1475–1485.
Mo, X., Rao, D. P., Kaur, K., Hassan, R., Abdel-Samea, A. S., Farhan, S. M., Bräse, S. & Hashem, H. (2024). *Molecules* **29**, 4770.
Mohanty, B. & Munshi, P. (2025). *Sci. Rep.* **15**, 45462.
Parsons, S., Flack, H. D. & Wagner, T. (2013). *Acta Cryst.* B**69**, 249–259.
Rigaku OD (2023). *CrysAlis PRO*. Rigaku Oxford Diffraction, Yarnton, Oxfordshire, England.
Rinderspacher, A., Gribble, G. W., Butcher, R. J. & Jasinski, J. P. (2007). *Acta Cryst.* E**63**, o671–o672.
Rivero-Crespo, M. A., Toupalas, G. & Morandi, B. (2021). *J. Am. Chem. Soc.* **143**, 21331–21339.
Sharma, S., Kumar, A. & Erande, R. D. (2024). *ChemistrySelect* ***9*** e202303476.
Sheldrick, G. M. (2015). *Acta Cryst.* C**71**, 3–8.
Shetty, S., Baig, N. & Alameddine, B. (2022). *Polymers* **14**, 4818.
Shibahara, F., Kanai, T., Yamaguchi, E., Kamei, A., Yamauchi, T. & Murai, T. (2014). *Chem. Asian J.* **9**, 237–244.
Shirani, H., Stensland, B., Bergman, J. & Janosik, T. (2006). *Synlett* 2459–2463.
Silveira, C. C., Mendes, S. R., Soares, J. R., Victoria, F. N., Martinez, D. M. & Savegnago, L. (2013). *Tetrahedron Lett.* **54**, 4926–4929.
Spackman, P. R., Turner, M. J., McKinnon, J. J., Wolff, S. K., Grimwood, D. J., Jayatilaka, D. & Spackman, M. A. (2021). *J. Appl. Cryst.* **54**, 1006–1011.
Wang, M. (2024). *Molecules* **29**, 5523.
Xalxo, A., Jyoti Goswami, U., Sarkar, S., Kandasamy, T., Mehta, K., Ghosh, S. S., Bharatam, P. V. & Khan, A. T. (2023). *Bioorg. Chem.* **141**, 106900.
Yuan, J., Xu, Z. & Wolf, M. O. (2022). *Chem. Sci.* **13**, 5447–5464.

supporting information

Acta Cryst. (2026). E**82**, 418-421 [https://doi.org/10.1107/S2056989026002872]

Crystal structure and Hirshfeld surface analysis of 3,3′-(sulfanediyl)bis(2-iodo-1-methyl-1*H*-indole)

Adisa Ayobami, Abid Shaikh and Clifford W. Padgett

Computing details

2-Iodo-3-[(2-iodo-1-methyl-1*H*-indol-3-yl)sulfanyl]-1-methyl-1*H*-indole

Crystal data

$C_{18}H_{14}I_2N_2S$
M_r = 544.17
Orthorhombic, *Fdd*2
a = 37.8416 (4) Å
b = 31.6009 (3) Å
c = 5.94404 (5) Å
V = 7108.05 (11) Å^3
Z = 16
F(000) = 4128
D_x = 2.034 Mg m^{-3}
Cu *Kα* radiation, *λ* = 1.54184 Å
Cell parameters from 7695 reflections
θ = 2.8–69.4°
μ = 28.89 mm^{-1}
T = 298 K
Needle, clear colourless
0.15 × 0.05 × 0.02 mm

Data collection

XtaLAB Synergy, Single source at home/near, HyPix3000 diffractometer
Radiation source: micro-focus sealed X-ray tube, PhotonJet (Cu) X-ray Source
Mirror monochromator
Detector resolution: 10.0000 pixels mm^{-1}
ω scans
Absorption correction: multi-scan (CrysAlisPro; Rigaku OD, 2023)
T_{min} = 0.401, T_{max} = 1.000
9127 measured reflections
2434 independent reflections
2352 reflections with $I > 2\sigma(I)$
R_{int} = 0.099
θ_{max} = 69.6°, θ_{min} = 3.7°
h = −45→39
k = −38→38
l = −7→5

Refinement

Refinement on F^2
Least-squares matrix: full
$R[F^2 > 2\sigma(F^2)]$ = 0.052
$wR(F^2)$ = 0.146
S = 1.18
2434 reflections
210 parameters
1 restraint
Hydrogen site location: inferred from neighbouring sites
H-atom parameters constrained
$w = 1/[\sigma^2(F_o^2) + (0.1145P)^2]$ where $P = (F_o^2 + 2F_c^2)/3$
$(\Delta/\sigma)_{max}$ = 0.001
$\Delta\rho_{max}$ = 0.90 e Å^{-3}
$\Delta\rho_{min}$ = −1.60 e Å^{-3}
Absolute structure: Flack *x* determined using 558 quotients $[(I^+)-(I^-)]/[(I^+)+(I^-)]$ (Parsons *et al.*, 2013)
Absolute structure parameter: −0.034 (16)

Special details

Geometry. All esds (except the esd in the dihedral angle between two l.s. planes) are estimated using the full covariance matrix. The cell esds are taken into account individually in the estimation of esds in distances, angles and torsion angles; correlations between esds in cell parameters are only used when they are defined by crystal symmetry. An approximate (isotropic) treatment of cell esds is used for estimating esds involving l.s. planes.

Fractional atomic coordinates and isotropic or equivalent isotropic displacement parameters (Å²)

	x	*y*	*z*	U_{iso}*/U_{eq}
I1	0.32692 (2)	0.48490 (2)	0.93756 (14)	0.0508 (3)
I2	0.43892 (2)	0.47566 (2)	0.71981 (17)	0.0578 (3)
S1	0.36946 (6)	0.53925 (8)	0.4606 (5)	0.0439 (6)
C5	0.2780 (3)	0.6351 (4)	0.230 (3)	0.061 (3)
H5	0.279642	0.654130	0.111082	0.073*
C14	0.3706 (3)	0.6641 (3)	0.938 (3)	0.055 (3)
H14	0.356860	0.688280	0.920913	0.066*
C7	0.2432 (3)	0.6070 (4)	0.538 (3)	0.052 (3)
H7	0.222570	0.606600	0.622775	0.062*
C16	0.4158 (3)	0.6273 (4)	1.158 (2)	0.052 (3)
H16	0.431069	0.625179	1.280030	0.063*
C9	0.2490 (3)	0.5395 (4)	0.926 (2)	0.047 (2)
H9A	0.245021	0.509541	0.927082	0.071*
H9B	0.227240	0.553922	0.894335	0.071*
H9C	0.257864	0.548363	1.069472	0.071*
C6	0.2476 (4)	0.6347 (4)	0.360 (3)	0.061 (3)
H6	0.229574	0.653719	0.326893	0.073*
C12	0.3896 (2)	0.5966 (3)	0.815 (2)	0.037 (2)
C13	0.3671 (3)	0.6333 (4)	0.786 (2)	0.050 (3)
H13	0.351147	0.635244	0.667507	0.060*
C18	0.4594 (4)	0.5450 (5)	1.140 (3)	0.067 (4)
H18A	0.480997	0.540454	1.058117	0.101*
H18B	0.452750	0.519378	1.215169	0.101*
H18C	0.462896	0.567063	1.248555	0.101*
N1	0.2752 (2)	0.5500 (3)	0.7496 (16)	0.0410 (18)
C17	0.4136 (3)	0.5951 (4)	0.998 (2)	0.043 (2)
C15	0.3947 (3)	0.6622 (4)	1.128 (2)	0.055 (3)
H15	0.395848	0.684538	1.229133	0.066*
C10	0.4193 (2)	0.5350 (3)	0.805 (2)	0.039 (2)
C11	0.3936 (2)	0.5572 (3)	0.697 (2)	0.039 (2)
C4	0.3058 (3)	0.6082 (3)	0.272 (2)	0.047 (3)
H4	0.326016	0.608604	0.182858	0.057*
C1	0.3086 (2)	0.5320 (3)	0.723 (2)	0.040 (2)
N2	0.4320 (2)	0.5572 (3)	0.986 (2)	0.047 (2)
C3	0.3025 (3)	0.5800 (3)	0.454 (2)	0.042 (2)
C2	0.3259 (2)	0.5495 (3)	0.550 (2)	0.039 (2)
C8	0.2712 (3)	0.5797 (3)	0.5853 (19)	0.039 (2)

Atomic displacement parameters (Å²)

	U^{11}	U^{22}	U^{33}	U^{12}	U^{13}	U^{23}
I1	0.0529 (4)	0.0460 (4)	0.0535 (5)	0.0002 (3)	−0.0029 (3)	0.0119 (3)
I2	0.0527 (4)	0.0459 (4)	0.0748 (6)	0.0076 (3)	0.0014 (4)	−0.0028 (4)
S1	0.0357 (10)	0.0523 (13)	0.0437 (14)	−0.0027 (10)	−0.0002 (10)	−0.0062 (12)
C5	0.067 (7)	0.046 (5)	0.069 (8)	−0.012 (5)	−0.021 (7)	0.020 (6)
C14	0.044 (5)	0.041 (5)	0.079 (9)	−0.008 (4)	0.023 (7)	0.002 (6)
C7	0.041 (5)	0.054 (6)	0.061 (7)	−0.001 (5)	−0.006 (5)	−0.009 (6)
C16	0.045 (5)	0.060 (6)	0.052 (7)	−0.012 (5)	0.001 (5)	−0.010 (6)
C9	0.040 (4)	0.060 (6)	0.042 (6)	−0.007 (5)	0.005 (5)	−0.003 (5)
C6	0.059 (6)	0.045 (6)	0.080 (10)	0.004 (5)	−0.028 (7)	−0.002 (6)
C12	0.031 (4)	0.037 (4)	0.043 (5)	−0.002 (3)	0.003 (4)	−0.006 (4)
C13	0.047 (6)	0.053 (6)	0.051 (7)	−0.023 (5)	0.017 (5)	−0.011 (5)
C18	0.067 (8)	0.064 (8)	0.071 (9)	0.014 (6)	−0.018 (8)	−0.009 (7)
N1	0.037 (4)	0.043 (4)	0.043 (5)	0.001 (3)	0.004 (4)	−0.001 (4)
C17	0.042 (4)	0.045 (5)	0.043 (6)	−0.006 (4)	0.000 (5)	0.001 (5)
C15	0.058 (6)	0.051 (6)	0.057 (8)	−0.012 (5)	0.004 (6)	−0.016 (6)
C10	0.033 (4)	0.031 (4)	0.054 (7)	0.002 (4)	0.007 (4)	0.001 (4)
C11	0.037 (4)	0.033 (4)	0.046 (6)	−0.002 (4)	0.002 (5)	−0.004 (4)
C4	0.048 (5)	0.042 (5)	0.051 (7)	−0.008 (5)	−0.004 (5)	0.007 (5)
C1	0.033 (4)	0.033 (4)	0.053 (6)	−0.007 (3)	−0.001 (5)	−0.004 (5)
N2	0.037 (4)	0.044 (4)	0.059 (6)	0.005 (4)	−0.006 (4)	0.001 (5)
C3	0.040 (4)	0.037 (4)	0.048 (6)	0.000 (4)	−0.001 (5)	0.000 (5)
C2	0.033 (4)	0.037 (5)	0.047 (6)	−0.012 (4)	−0.010 (4)	0.005 (5)
C8	0.038 (4)	0.031 (4)	0.047 (5)	0.002 (4)	−0.006 (4)	−0.004 (4)

Geometric parameters (Å, º)

I1—C1	2.079 (12)	C6—H6	0.9300
I2—C10	2.080 (9)	C12—C13	1.448 (17)
S1—C11	1.770 (11)	C12—C17	1.418 (16)
S1—C2	1.761 (11)	C12—C11	1.436 (13)
C5—H5	0.9300	C13—H13	0.9300
C5—C6	1.39 (2)	C18—H18A	0.9600
C5—C4	1.375 (18)	C18—H18B	0.9600
C14—H14	0.9300	C18—H18C	0.9600
C14—C13	1.336 (17)	C18—N2	1.435 (17)
C14—C15	1.452 (19)	N1—C1	1.393 (12)
C7—H7	0.9300	N1—C8	1.364 (14)
C7—C6	1.38 (2)	C17—N2	1.390 (14)
C7—C8	1.394 (15)	C15—H15	0.9300
C16—H16	0.9300	C10—C11	1.361 (14)
C16—C17	1.392 (16)	C10—N2	1.369 (16)
C16—C15	1.373 (19)	C4—H4	0.9300
C9—H9A	0.9600	C4—C3	1.409 (16)
C9—H9B	0.9600	C1—C2	1.342 (17)
C9—H9C	0.9600	C3—C2	1.428 (14)

C9—N1	1.476 (14)	C3—C8	1.417 (15)
C2—S1—C11	100.6 (5)	C1—N1—C9	126.6 (9)
C6—C5—H5	119.0	C8—N1—C9	126.0 (9)
C4—C5—H5	119.0	C8—N1—C1	107.4 (9)
C4—C5—C6	121.9 (12)	C16—C17—C12	122.7 (10)
C13—C14—H14	118.1	N2—C17—C16	129.3 (11)
C13—C14—C15	123.8 (12)	N2—C17—C12	108.0 (10)
C15—C14—H14	118.1	C14—C15—H15	120.0
C6—C7—H7	121.5	C16—C15—C14	120.0 (11)
C6—C7—C8	117.0 (12)	C16—C15—H15	120.0
C8—C7—H7	121.5	C11—C10—I2	127.2 (9)
C17—C16—H16	121.3	C11—C10—N2	111.0 (9)
C15—C16—H16	121.3	N2—C10—I2	121.9 (7)
C15—C16—C17	117.5 (12)	C12—C11—S1	127.6 (8)
H9A—C9—H9B	109.5	C10—C11—S1	125.4 (8)
H9A—C9—H9C	109.5	C10—C11—C12	107.0 (10)
H9B—C9—H9C	109.5	C5—C4—H4	121.2
N1—C9—H9A	109.5	C5—C4—C3	117.5 (12)
N1—C9—H9B	109.5	C3—C4—H4	121.2
N1—C9—H9C	109.5	N1—C1—I1	121.7 (8)
C5—C6—H6	119.0	C2—C1—I1	127.0 (7)
C7—C6—C5	122.1 (11)	C2—C1—N1	111.3 (10)
C7—C6—H6	119.0	C17—N2—C18	124.2 (11)
C17—C12—C13	119.5 (10)	C10—N2—C18	128.0 (9)
C17—C12—C11	106.2 (9)	C10—N2—C17	107.8 (9)
C11—C12—C13	134.3 (10)	C4—C3—C2	132.7 (11)
C14—C13—C12	116.5 (13)	C4—C3—C8	120.1 (10)
C14—C13—H13	121.8	C8—C3—C2	107.2 (10)
C12—C13—H13	121.8	C1—C2—S1	127.9 (8)
H18A—C18—H18B	109.5	C1—C2—C3	106.3 (9)
H18A—C18—H18C	109.5	C3—C2—S1	125.8 (9)
H18B—C18—H18C	109.5	C7—C8—C3	121.4 (10)
N2—C18—H18A	109.5	N1—C8—C7	130.8 (11)
N2—C18—H18B	109.5	N1—C8—C3	107.8 (9)
N2—C18—H18C	109.5		
I1—C1—C2—S1	−2.6 (15)	C17—C12—C11—C10	−1.5 (12)
I1—C1—C2—C3	179.6 (8)	C15—C14—C13—C12	−1.3 (16)
I2—C10—C11—S1	2.4 (15)	C15—C16—C17—C12	−2.7 (17)
I2—C10—C11—C12	−179.0 (7)	C15—C16—C17—N2	179.0 (11)
I2—C10—N2—C18	0.6 (18)	C11—S1—C2—C1	−64.1 (11)
I2—C10—N2—C17	−179.7 (7)	C11—S1—C2—C3	113.3 (10)
C5—C4—C3—C2	−177.0 (12)	C11—C12—C13—C14	178.3 (11)
C5—C4—C3—C8	0.6 (16)	C11—C12—C17—C16	−176.7 (10)
C16—C17—N2—C18	−3 (2)	C11—C12—C17—N2	1.9 (12)
C16—C17—N2—C10	176.9 (11)	C11—C10—N2—C18	−179.0 (13)
C9—N1—C1—I1	0.9 (14)	C11—C10—N2—C17	0.7 (13)

C9—N1—C1—C2	−178.3 (10)	C4—C5—C6—C7	−1 (2)
C9—N1—C8—C7	−0.2 (18)	C4—C3—C2—S1	1.5 (18)
C9—N1—C8—C3	179.3 (10)	C4—C3—C2—C1	179.4 (11)
C6—C5—C4—C3	−0.3 (19)	C4—C3—C8—C7	0.1 (16)
C6—C7—C8—N1	178.5 (11)	C4—C3—C8—N1	−179.5 (10)
C6—C7—C8—C3	−1.0 (17)	C1—N1—C8—C7	−179.0 (11)
C12—C17—N2—C18	178.1 (12)	C1—N1—C8—C3	0.6 (11)
C12—C17—N2—C10	−1.6 (12)	N2—C10—C11—S1	−178.0 (8)
C13—C14—C15—C16	0.7 (18)	N2—C10—C11—C12	0.6 (12)
C13—C12—C17—C16	2.1 (16)	C2—S1—C11—C12	−48.3 (10)
C13—C12—C17—N2	−179.3 (9)	C2—S1—C11—C10	130.0 (10)
C13—C12—C11—S1	−1.5 (18)	C2—C3—C8—C7	178.3 (10)
C13—C12—C11—C10	180.0 (11)	C2—C3—C8—N1	−1.3 (12)
N1—C1—C2—S1	176.6 (8)	C8—C7—C6—C5	1.3 (19)
N1—C1—C2—C3	−1.3 (13)	C8—N1—C1—I1	179.7 (7)
C17—C16—C15—C14	1.3 (17)	C8—N1—C1—C2	0.5 (12)
C17—C12—C13—C14	−0.1 (15)	C8—C3—C2—S1	−176.3 (8)
C17—C12—C11—S1	177.0 (8)	C8—C3—C2—C1	1.6 (12)